JOURNAL OF AGRICULTURAL AND FOOD CHEMISTRY

Bioactive Constituents, Metabolites, and Functions

Hepatic Lipidomics Analysis Reveals the Anti-obesity and Cholesterol-lowering Effects of Tangeretin in High-Fat Diet-Fed Rats

Konglong Feng, Yaqi Lan, Xiaoai Zhu, Jun Li, Tong Chen, Qingrong Huang, Chi-Tang Ho, Yunjiao Chen, and Yong Cao

J. Agric. Food Chem., **Just Accepted Manuscript** • Publication Date (Web): 12 May 2020

Just Accepted

is published by the American Chemical Society. 1155 Sixteenth Street N.W., Washington, DC 20036

Hepatic Lipidomics Analysis Reveals the Anti-obesity and Cholesterol-lowering Effects of Tangeretin in High-Fat Diet-Fed Rats

Konglong Feng,[†] Yaqi Lan,[†] Xiaoai Zhu,[†,§] Jun Li,[†] Tong Chen,[†,‡] Qingrong Huang,[#] Chi-Tang Ho,[#] Yunjiao Chen,[†,*] Yong Cao,[†,*]

[†]Guangdong Provincial Key Laboratory of Nutraceuticals and Functional Foods, College of Food Sciences, South China Agricultural University, Guangzhou, Guangdong 510642, China

[§]School of Food Science and Technology, Henan University of Technology, Zhengzhou, Henan 450001, China

[‡]Shenzhen Agricultural Product Quality Safety Inspection Testing Center, Shenzhen, Guangdong 518000, China

[#]Department of Food Science, Rutgers University, 65 Dudley Road, New Brunswick, New Jersey 08901, USA

[*] Corresponding authors:

Yong Cao, Fax (Tel.): +86(020)8586234, E-mail: caoyong2181@scau.edu.cn.

Yunjiao Chen, Fax (Tel.): +86(020)8586234, E-mail: yunjiaochen@scau.edu.cn.

ABSTRACT: Tangeretin (TAN) exhibited anti-lipogenic, anti-diabetic and lipid-lowering effects. However, the lipid biomarkers and underlying mechanisms for anti-obesity and cholesterol-lowering effects of TAN have not been sufficiently investigated. Herein, we integrated biochemical analysis with lipidomics to elucidate its efficacy and mechanisms in high-fat diet-fed rats. TAN at supplementation levels of 0.04% and 0.08% not only significantly decreased body weight gain, serum total cholesterol and low-density lipoprotein cholesterol levels but also ameliorated hepatic steatosis. These beneficial effects were associated with the declining levels of fatty acids, diacylglycerols (DG), triacylglycerols, ceramides and cholesteryl esters by hepatic lipidomics analysis, which were attributed to downregulating lipogenesis related-genes and upregulating lipid oxidation- and bile acid biosynthesis-related genes. Additionally, 21 lipids were identified as potential lipid biomarkers, such as DGs and phosphatidylethanolamines. These findings indicated that the modulation of lipid homeostasis might be the key pathways for the mechanisms of TAN in the anti-obesity and cholesterol-lowering effects.

KEYWORDS: Tangeretin, Anti-obesity, Cholesterol-lowering, Lipidomics, Diacyglycerols

INTRODUCTION

Tangeretin (TAN), 4',5,6,7,8-pentamethoxyflavone, is one of the most common and abundant polymethoxyflavones (PMFs) found exclusively in citrus peel.[1] Tangeretin has attracted much research interest due to their good safety and various beneficial bioactivities, such as anti-lipogenic, anti-diabetic, antihypertensive, antiviral, antioxidant, anti-inflammatory, hepatoprotective activities, and regulation of lipid metabolism.[2-9] Kurowska et al.[10] reported that TAN regulated apoB-containing lipoprotein metabolism in HepG2 cells, suggesting that it has potential therapeutic applications in hypertriglyceridemia. Furthermore, subsequent *in vivo* studies demonstrated that TAN exhibited lipid-lowering effects, which were associated with its extensive absorption and metabolism, but the underlying mechanisms were unknown.[11] It was reported that citrus peel extracts with a high content of TAN could prevent obesity by modulating gut microbiota and could be a candidate for fighting obesity.[12] Recently, citrus PMFs containing 15.62% TAN represented potential lipid-lowering effects by down-regulating the mTOR/P70S6K/SREBP pathway in human liver HL-7702 cells, and might strongly improve diet-induced obesity, hepatic steatosis and dyslipidemia in a gut microbiota-dependent manner.[9] Although the anti-obesity, hypolipidemic and regulation of lipid metabolism effects of PMFs as a group of compounds have been widely reported, these effects of individual TAN and their precise biochemical mechanisms have not been fully studied.

Lipids are important components required for keeping various homeostatic,

physiologic and cellular processes in the body.[13] Furthermore, the dysregulation of lipid metabolism results in many major health problems, such as obesity and non-alcoholic fatty liver disease (NAFLD), while traditional clinical techniques are insufficient to characterize. Lipidomics, a novel omics strategy, is capable to investigate lipid metabolism by determining lipid composition and identifying lipid biomarkers at a molecular level.[14-15] More recently, a lipidomics approach has been used to assess the biological activity of natural medicines and functional foods.[16-17] Lipidomics analysis demonstrated the lipid-lowering effects of arabinoxylan associated with the lowering levels of some free fatty acids (FFA), 12α-hydroxylated bile acids, and carnitines (CAR) on type 2 diabetic rats, but an increase of lysophosphatidylcholines (LPC) levels.[18] Wen et al.[19] demonstrated that polysaccharides from fermented *Momordica charantia* could inhibit obesity by improving the lipid metabolism with the decrease of FFAs and monoacylglycero-phosphoserines. Lipidomics has also been employed to study the underlying molecular mechanism of the beneficial effects of dietary ω-3 polyunsaturated fatty acids.[20] Nowadays, through the overall and systematic quantitative analysis of multifarious lipid species, we could assign the functions of lipids as signaling molecules and regulations of metabolic pathways, as well as elucidate the interplays between nutrients and human metabolism.[14,20] Therefore, lipidomics can act an important part in mechanistic studies of nutrition research. Obviously, the anti-obesity and hypolipidemic effect of PMFs have been well proved, and gene expressions and gut microbiota involved in lipid metabolism were also

64 investigated to explain changes for identifying the underlying mechanisms.[12,21-23]
65 However, so far none of the studies have applied lipidomics to investigate the efficacy
66 of TAN and elucidate the lipid biomarkers responsible for the bioactivities of TAN.

67 In this study, high purity TAN was isolated and purified from tangerine peel oil
68 (TPO) by using multistep isolation and recrystallization. Subsequently, we integrated
69 biochemical analysis with lipidomics profiling to elucidate the effect and molecular
70 mechanisms of the anti-obesity and cholesterol-lowering in the regulation of lipid
71 metabolism after supplementing with TAN in high-fat diet-fed rats.

72

73 **METHODS AND MATERIALS**

74 **Materials and chemicals**. The tangerine peels from different origins were obtained
75 from Guangdong Provincial Key Laboratory of Nutraceuticals and Functional Foods
76 (Table S1). TAN, nobiletin (NOB), and 3,5,6,7,8,3',4'-heptamethoxyflavone (HMF)
77 (purity>98%) were supplied by Shanghai Yuanye Bio-Technology Co., Ltd. (Shanghai,
78 China). Serum biochemistry kits for determining the levels of serum high-density
79 lipoprotein cholesterol (HDL-C), low-density lipoprotein cholesterol (LDL-C), total
80 triglyceride (TG), total cholesterol (TC), alanine transaminase (ALT) and aspartate
81 transaminase (AST) were supplied by Nanjing Jiancheng Bio-Engineering Institute Co.,
82 Ltd. (Nanjing, China). RNAprep Pure Tissue Kit and FastKing RT Kit were supplied
83 by Tiangen Biotech Ltd. (Beijing, China). iTaqTM Universal SYBR® Green Supermix
84 was obtained from Bio-Rad (Hercules, CA, USA).

Extraction and selection of tangerine peel oil. The dried tangerine peels (40 mesh, 10 kg) from different origins were crushed, sifted and put in a self-developed continuous phase transition extraction equipment.[24] The extraction was performed at a temperature of 30 °C for 60 min and a pressure of 0.6 MPa by utilizing *n*-butane as the solvent, and then n-butane and extracted TPO were separated at 70 °C. Subsequently, we firstly determined the contents of major PMFs (TAN, NOB and HMF) in the obtained TPO samples by HPLC analysis, and selected the one is rich in TAN for further isolation and purification.

Simultaneous separation and purification of NOB and TAN. TPO sample 19 with the content of TAN up to 38.79 mg/mL, was selected for further isolation and purification of TAN. The separation and purification of NOB and TAN by multistep separation and recrystallization was carried out referring to our previous method with modification.[21] The procedures were as follows: Step 1: A 10-fold volume of petroleum ether was added into TPO and then the mixtures were stirred and lay it overnight at 4 °C. The insoluble brown TPO precipitate was obtained by centrifuged at 2000g for 10 min, and then removed essential oils and other petroleum ether soluble contaminants by rinsing with petroleum ether. Similarly, the precipitate was repeatedly subject to another rinse process by adding 30% methanol at about a ratio of 1:4 to remove other impurities including the remaining essential oil and petroleum ether. The yellowish-brown residue was obtained through centrifugation and dry. Step 2: The yellowish-brown residue was dissolved in ethyl acetate by boiling and immediately filtrated to

remove insoluble impurities. The proper additive proportion of ethyl acetate was based on the content of TAN in the residue. The filtrate was subjected to slowly cool at room temperature to facilitate crystal formation. After that the filtrate A and precipitate A were obtained by vacuum filter. Step 3: The precipitate A was repeatedly subject to step 2 to obtain the filtrate B and precipitate B. Subsequently, the filtrate A and the filtrate B were combined and then solvents evaporated. Step 4: After the evaporation and desiccation, the yellow precipitate C was collected and then completely dissolved at 80 °C temperature for 40 min by adding 20%-30% methanol at about a ratio of 1:100. The mixture was immediately filtrated and allowed to keep at temperature of 60 °C for 4-8 h to promote crystal formation. After crystallization, the pale yellow crystals of TAN were obtained by a vacuum filter and followed by twice washes with 30% methanol and dry. Eventually, the white crystals of TAN were again recovered through a repetitive step of crystallization and then were determined by HPLC. Step 5: The precipitate B was subjected to dissolve, crystallize at room temperature, filter, wash and dry according to step 4. After crystallization, the pale yellow crystals of NOB were obtained.

HPLC analysis. The contents of major PMFs (TAN, NOB and HMF) in 22 TPO samples, the white crystals of TAN and the pale yellow crystals of NOB were determined using a Shimadzu LC-15C HPLC system (Shimadzu, Japan) equipped with an DIKMA's Diamonsil C18 column (250 mm × 4.6 mm id, 5 μm). The analytical conditions of HPLC-PDA were presented as described in our previous study with minor

127 modifications.[21] However, the elution gradient was optimized as below : 0–6 min, 60%–
128 65% B; 6–11 min, 65%–70% B; 11–20 min, 70% B.

129 **Animals experimental design and sample collection.** Male Sprague–Dawley (SD)
130 rats (100-150 g, 6 weeks old) were supplied by the Guangdong Medical Laboratory
131 Animal Center (Guangzhou, China) and fed under specific-pathogen-free (SPF)
132 conditions. All procedures were managed on the basis of the protocol (SCAU-AEC-
133 2010-0416) which was authorized by the Animal Ethics Committee of South China
134 Agricultural University. After adaptive feeding for 2 weeks, the rats were randomly
135 divided into normal diet group (ND), high-fat diet group (HFD), high-fat diet with 0.02%
136 TAN group (HFD+LTAN), high-fat diet with 0.04% TAN group (HFD+MTAN), high-
137 fat diet with 0.08% TAN group (HFD+HTAN). The detailed components of
138 experimental diets are shown in Table S2. All rats were given free access to food and
139 water. The daily food intake, food efficiency ratio and body weight were recorded once
140 a week.

141 At the end of the 6-weeks experiment, all rats were anesthetized with sodium
142 pentobarbital after fasting for 12 h. Blood was collected from the abdominal aorta and
143 then centrifugated at 1000g for 20 min at 4 ℃ to get supernatant serum samples. The
144 organ and adipose tissue were individually collected and weighed after sacrifice. All
145 samples were rapidly frozen in liquid nitrogen and then stored in −80 ℃. A part of liver
146 tissue was fixed in a 10% buffered formalin for hepatic histological analysis.

147 **Biochemical analysis and hepatic histological analysis.** The serum concentrations of

148 TC, TG, HDL-C, LDL-C, ALT and AST were determined using serum biochemistry
149 kits referring to manufacturer's instruction. The procedures of hematoxylin and eosin
150 staining (H&E) were obtained referring to our previous report.[21]
151 **Liver lipidomics analysis.** The total lipids were extracted from the liver in the ND,
152 HFD and HFD+HTAN groups (n=4) referring to the method of Feng et al.[25] with some
153 modifications. Liver tissues (50 mg) were homogenized in a 1 mL mixture (include
154 methanol, MTBE and internal standard mixture). After homogenization, the mixture
155 was vortexed and then centrifuged for 10 min at 13680 xg at 4 °C. 500 μL supernatant
156 was collected and evaporated to dryness under a stream of N_2. Finally, the lipid extracts
157 were redissolved in a mixture of acetonitrile/isopropanol (1/9, V/V) containing 0.04%
158 acetic acid and 5 mmol/L ammonium formate for LC-MS/MS analysis.
159 Hepatic lipidomics profiling was performed by using an LC-ESI-MS/MS system
160 (HPLC, Shim-pack UFLC SHIMADZU CBM30A system; MS, Applied Biosystems
161 4500 Q TRAP). Samples (2 μL) were separated on Thermo Scientific™ Acclaim™ C30
162 column (2.6 μm, 2.1 mm×100 mm, Sunnyvale, CA, USA) with a flow rate of 0.35
163 mL/min and column temperature of 45 °C. The mobile phases consisted of a mixture
164 of acetonitrile/water (60:40, V/V) (A) and a mixture of acetonitrile/isopropanol (10:90,
165 V/V) (B), both containing 0.04% acetic acid and 5 mmol/L ammonium formate. The
166 elution gradient was set stepwise as follows: 0–3 min, 20%–50% B; 3–5 min, 50%–65%
167 B; 5–9 min, 65%–75% B; 9–15.5 min, 75%–90% B. The qualitative and quantitative
168 analysis of lipid profiling was performed by utilizing multiple reaction monitoring

(MRM) analysis at Wuhan MetWare Biotechnology Co., Ltd. The analytical conditions and detailed work parameters were presented as described in reported literatures.[19,26]

Determination of mRNA expression levels by qRT-PCR. Total mRNA was extracted from the liver in the ND, HFD and HFD+HTAN groups (n=6) respectively according to the instruction of RNAprep Pure Tissue Kit (Tiangen Biotech Ltd., Beijing, China) and then first-strand cDNA was synthesized as described previously.[27] The levels of cDNA encoding genes participated in lipid metabolism were quantified using iTaqTM Universal SYBR® Green Supermix and a LightCycler 480 II detection system (Roche Diagnostics, Indianapolis, IN.). The PCR primer sequences are shown in Table S3.

Statistical analysis. All data were shown as mean ± SD. Multiple comparison among groups was carried out by using Duncan's multiple range test in ANOVA analysis. The lipids data were analyzed by using the Analyst 1.6.1 software (AB SCIEX, Toronto, Ontario, Canada). The significantly differential lipid species among experimental groups were screened out according to the variable importance in the projection (VIP > 1) from the orthogonal partial least-squares discriminant analysis (OPLS-DA) model and fold change (FC $\geqslant$ 2 or $\leqslant$ 0.5).

RESULTS

Simultaneous separation and purification of NOB and TAN by multistep separation and recrystallization. In order to efficiently obtain large amounts of TAN from the TPO, we firstly determined the content of PMFs in 22 TPO samples from

different origins and selected the one rich in TAN for further isolation and purification. As shown in Figure 1A and D, NOB, HMF and TAN were identified as the main PMFs constituents in TPO. Among these TPO samples, TPO sample 19 from Guangxi province contained the highest content of TAN (38.79 mg/mL), and the maximum yield of PMFs was up to 85.13 mg/mL. Hence, TPO sample 19 was selected for isolation and purification of TAN. The procedures of simultaneous separation and purification of NOB and TAN are shown in Figure 1B. Firstly, the crude extract of PMFs was isolated from TPO sample 19, in which the proportion of combined NOB and TAN increased from 9.68% to 56.88%. Subsequently, we respectively separated NOB and TAN from the crude extract of PMFs by adding the proper additive proportion of ethyl acetate to dissolve and then the NOB precipitation occurred in the earlier stage of crystallizing, while a large proportion of TAN dissolved in the filtrate. Finally, the higher purities of TAN (96.17%) were obtained through recovering the filtrate containing a large proportion of TAN and a repetitive step of crystallization. Similarly, the higher purities of NOB (95.75%) were obtained. The higher purities of TAN white crystals were used for further study.

Effect of TAN supplementation on body weight, food efficiency ratio and fat mass. To address whether TAN exhibits an anti-obesity effect, we used SD rats fed HFD as an obesity model. After feeding a high-fat diet (HFD) for consecutive 6 weeks in rats, the final body weight, body weight gain and relative adipose tissue weights were higher than those of rats fed with the normal diet, along with higher calorie intake and food

211 efficiency ratio ($p < 0.05$). These results indicated that the obesity model was triggered
212 by feeding an HFD (Table 1). Interestingly, when contrasted with the HFD-alone group,
213 the HFD+MTAN and HFD+HTAN groups markedly reduced final body weight, body
214 weight gain and food efficiency ratio ($p < 0.05$) with no apparent changes in daily
215 energy intake. Moreover, rats in HFD+MTAN and HFD+HTAN groups exhibited a
216 striking decrease in the weight of perirenal, epididymal adipose, and visceral adipose
217 tissue than those fed HFD-alone ($p < 0.05$) (Table 2). Though consumption of TAN
218 could decrease body weight gain, food efficiency ratio and relative adipose tissue
219 weights in a dose-dependent manner, the result in a low dose of TAN group
220 (HFD+LTAN) was not statistically significant ($p > 0.05$). Five groups had no apparent
221 differences in the organ weights except the liver, suggesting that rats fed an HFD did
222 not show organ injury and TAN has no obvious side effects, which was in accordance
223 with the previous study.[2] On the basis of these data, consumption of 0.04% and 0.08%
224 TAN could effectively reduce weight gain and fat accumulation of rats by lowering
225 food availability.

226 **Effect of TAN supplementation on serum biochemistry.** The effects of TAN
227 supplementation on serum TC, TG, HDL-C, LDL-C, ALT and AST levels are presented
228 in Figure 2. It showed that the rats in the HFD group showed dyslipidemia, which
229 characterized by an increment in serum TC, TG and LDL-C concentrations in contrast
230 to the ND group ($p < 0.05$), but a reduction in serum HDL-C level. Interestingly, TAN
231 supplementation significantly lowered serum TC and LDL-C levels in contrast to the

HFD-alone group ($p < 0.05$), but did not affect the serum TG and HDL-C levels. Meanwhile, no apparent differences in the levels of serum ALT and AST were observed among the five groups.

Effect of TAN supplementation on the hepatic steatosis induced by a high-fat diet. HFD led to a remarkably increased liver index of rats and yellowish-orange and pale fatty livers. Moreover, the HFD-alone rats exhibited higher liver TG and TC levels and revealed a large amount of lipid droplet accumulation in the liver by observation of H&E staining (Figure 3). However, when contrasted with the HFD group, the hepatic weights and the levels of hepatic TG and TC were remarkably reduced in the HFD+MTAN and HFD+HTAN groups ($p < 0.05$). Histological analysis of hepatic tissue exhibited that supplementation of TAN attenuated degree of liver steatosis with the reduction of macrovesicular steatosis and recovery of a typical structure of hepatic lobules and hepatic cell (Figure 3D). These results implied that consumption of TAN might be effectively declined lipid droplet accumulation in liver and improved hepatic steatosis.

TAN supplementation improved lipid metabolism in the liver by lipidomics analysis. To further investigate whether the lipid biomarkers are responsible for the bioactivities of TAN, we analyzed the differences in lipid composition based on the lipidomics approach. A total of 791 lipid metabolites were identified in the liver tissues from ND, HFD and HFD+HTAN groups, including 245 TGs, 53 DGs, 37 FFAs, 38 ceramides (CER), 19 cholesteryl esters (CE), 131 phosphatidylcholines (PC), 102

253 phosphatidylethanolamines (PE), and others (Supplemental file 1). As shown in Figure
254 4 A-C, the total contents of TGs, DGs, FFAs, CEs, CERs, PSs, PIs, PGs, PAs, and LPSs
255 in the HFD group were remarkably enhanced in contrast to the ND group ($p < 0.05$),
256 implying that an HFD led to a severe disturbance of lipid metabolism in rats.
257 Interestingly, supplementation of TAN improved the disorder of lipid metabolism
258 induced by an HFD with a remarkable decrease in contents of these lipid species except
259 for PSs and LPSs ($p < 0.05$). To obtain comparative interpretations and investigate
260 variation among groups, principal components analysis (PCA) was performed and
261 shown in Figure 4D. It was observed that the HFD group clearly distinguished from the
262 ND group, while the HFD+HTAN group separated away from the HFD group and
263 aggregated close to the ND group, suggesting that the consumption of TAN improved
264 the disordered metabolisms toward the normal condition. Likewise, a heatmap revealed
265 that the lipid metabolites patterns in the HFD group were different in contrast to the ND
266 group, but these patterns were partially improved by TAN supplementation
267 (Supplementary file 2).

268 **TAN supplementation altered the important differential lipid species in the liver.**
269 We obtained two multivariate OPLS-DA models with validation parameters of fitness
270 (R2X = 0.679 and R2Y = 1) and predictability (Q2 = 0.982) in ND versus HFD, as well
271 as fitness (R2X = 0.445 and R2Y = 0.99) and predictability (Q2 = 0.869) in HFD versus
272 HFD+HTAN, respectively. The results indicated that OPLS-DA models shown a
273 goodness of fit and could be considered as a predictable model to competently evaluate

the variation in lipidomics profiles. A clear separation of the OPLS-DA score plot is exhibited in ND versus HFD and HFD versus HFD+HTAN, respectively in Figure 5 A&B, suggesting that lipid metabolic perturbations were induced by an HFD and intervened by TAN. Volcano plot analysis was applied to screen out as lipid biomarker candidates accounting for such distinction. Using the criteria of FC $\geqslant$ 2 or $\leqslant$ 0.5 and VIP$\geqslant$ 1, 322 significantly differential lipid species were identified in ND versus HFD (Figure 5C). As shown in the heatmap (Figure 6), of the 322 identified lipids, the levels of 288 lipid species from seven major lipid classes in the HFD group, including TGs, DGs, FFAs, CEs, CERs, PSs and PGs, were markedly enhanced as compared with ND group. Whereas the significantly downregulated lipid species were mainly enriched in eicosanoid, LPC and PC classes. Notably, 25 lipids significantly changed between HFD and HFD+HTAN groups in Figure 5D, and most of them were remarkably downregulated. In addition, the differences in the levels of the potential lipid biomarkers among three groups were displayed in Figure 5 E&F. The contents of two TGs (TG (18:2/18:3/20:4) and TG (18:0/20:4/22:6)), six DGs (DG (16:0/22:4), DG (18:1/20:3), DG (18:4/18:1), DG (18:1/22:4), DG (18:1/20:5) and DG (18:1/22:5)), five FFAs (FFA (14:1), FFA (18:4), FFA (20:5), FFA (22:5) and FFA (24:5)), Eicosanoid (9,10-DiHOME), three CARs (myristoyl-carnitine, tetradecenoyl-carnitine and palmitodileoyl-carnitine), three PEs (PE (14:0/18:1), PE (18:1/18:0) and PE (18:1/18:1)), and PG (18:2/18:0) in the HFD group were markedly enhanced in contrasted to the ND group, while TAN supplementation remarkably decreased the

295 contents of these lipids ($p < 0.05$). Although the contents of palmitoleoyl-carnitine, PC
296 (O-20:2/22:1) and PE (18:0/18:3) were remarkably lowered in the HFD+HTAN group
297 but were not affected between ND and HFD groups. Thus, these results indicated that
298 these 21 lipids included 2 TGs, 6 DGs, 5 FFAs, 1 eicosanoid, 3 CARs, 3 PEs and 1 PG
299 might be represented potential biomarkers responsible for the lipid-lowering effects of
300 TAN.

301 **Pathway Analysis.** Pathways enrichment analysis could provide some clues to the
302 biochemical and signal transduction pathways that significantly differential lipid
303 species might involve in. As shown in Figure 7, the rats fed HFD were clearly damaged
304 the pathways of glycerolipid metabolism, cholesterol metabolism, fat digestion and
305 absorption, thermogenesis, and regulation of lipolysis in adipocytes as compared with
306 the normal diet group, whereas TAN supplementation ameliorated the pathways of
307 glycerophospholipid metabolism, glycerolipid metabolism, fatty acid degradation, fatty
308 acid elongation, AMPK signaling pathway, and NAFLD.

309 **Effects of TAN supplementation on the expression of genes participated in lipid**
310 **metabolism in livers.** To determine the underlying mechanism about the improvement
311 of abnormal lipid metabolism, we further assessed the transcription levels of genes
312 participated in lipid metabolism by qRT-PCR (Figure 8A). As compared with the ND
313 group, the expression levels of adipogenic genes, including *AMPK*, *SREBP-1c*, *ACC*,
314 *FAS* and *SCD1*, were markedly disrupted in the HFD group ($p < 0.05$). In contrast, the
315 gene expression levels of *SREBP-1c*, *ACC*, *FAS* and *SCD1* in the HFD+HTAN group

were remarkably lower than those of HFD group, but the lipolysis genes *AMPK* and *CPT1* expression levels were remarkably raised ($p < 0.05$). In addition, supplementation of TAN markedly upregulated the expression of *CYP7A1* and *CYP27A1* ($p < 0.05$), which are participated in bile acid metabolism, but the expression levels of genes *PPARα*, *PPARγ* and *LXRα* were unchanged in contrast to the HFD group.

DISCUSSION

Given the magnitude of obesity incidence and its related metabolic diseases, it is not surprising that epidemiological studies have demonstrated that a high intake of flavonoid-rich foods exhibits anti-obesity and hypolipidemic effects.[28] Citrus PMFs are of great interest because of their potential efficacy in anti-obesity and regulation of metabolic disorder and lipid metabolism.[29] A previous study simply first reported the lipid-lowering effect of TAN, while TAN had no effect on body weight.[11] However, we found that TAN at supplementation levels of 0.04% and 0.08% (the dose of approximately 6.8 and 13.6 mg/kg for human, respectively) not only remarkably reduced body weight gain, body fat, serum TC and LDL-C concentrations with no effect on serum TG and HDL-C concentrations, but also ameliorated hepatic steatosis by notably decreasing the liver weight increments, hepatic TC and TG levels. Although previous studies also found that TAN altered weight gain, and lowered the serum TG, TC and LDL-C concentrations in streptozotocin-induced diabetic rats, these studies were more focused on the anti-diabetes effect of TAN.[4,30] In the present study, we found

that TAN at supplementation levels of 0.08% could prevent obesity, dyslipidemia and hepatic steatosis by downregulating the lipogenesis-related genes (*SREBP-1c*, *ACC* and *FAS*) and upregulating the genes participated in lipid oxidation (*AMPK* and *CPT1*). Lee et al.[31] found that 100 mg/kg of NOB dramatically ameliorated obesity and insulin resistance by up-regulating adipogenesis genes *PPAR γ*, *SREBP-1c*, *FAS* and *SCD-1* and down-regulating the genes involved in energy expenditure *PPARα*, *CPT-1* and *UCP-2*. Besides, the aged citrus peel extract remarkably decreased HFD-induced obesity and hepatic steatosis by mediating the AMPK pathway.[32] Moreover, we have previously demonstrated that HMF could ameliorate obesity and hyperlipidemia by increasing the mRNA expression levels of genes *Cpt1b*, *Crat*, *Cd36*, *Slc27a5* and *Ucp3*, and reducing the mRNA expression levels of genes *Srebp1c* and *Fasn*.[21] Taken together, most of PMFs could prevent obesity, dyslipidemia and hepatic steatosis mainly attributing to inhibit fatty acid synthesis and adipogenesis, as well as enhance fatty acid oxidation.[8,22,33] Our studies were also in agreement with these conclusions.

The dysregulation of lipid metabolism is a hallmark of various metabolic disorders, which will lead to inefficient lipid metabolism, thereby inducing the development of obesity and dyslipidemia.[34-35] The liver, as an important organ of energy metabolism, maintains lipid homeostasis via regulating the synthesis and catabolism of lipids such as FFAs, TGs and cholesterol. Lipids metabolism disorders in the liver provide the ‘‘first hit’’ in the progress of hepatic steatosis.[36] Hence, in this study, the application of lipidomic analysis in the liver could provide new insights into studying lipid

358 metabolism in obesity, dyslipidemia and fatty liver so as to understand the molecular
359 mechanisms in the anti-obesity and cholesterol-lowering effect of TAN. Analysis of
360 total lipid contents in livers found that when contrasted with the ND group, a
361 remarkable increase in the contents of TGs, DGs, FFAs, CEs, CERs, PSs, PIs, PGs, PAs,
362 and LPCs were discovered in the HFD group. Similar observations were reported by
363 Feng et al.[37] While supplement with 0.08% TAN showed a clear tendency to have lower
364 contents of these lipid species except PSs and LPSs in lipidomic profiles, indicating
365 TAN could improve an imbalance between the lipid synthesis and catabolism induced
366 by an HFD. The storage of FFAs not only can facilitate abnormal accumulation of TG
367 in the hepatic cell but also can be transformed into lipid intermediates, such as DGs and
368 CERs, to damage cellular functions and lead to lipotoxicity, thereby developing hepatic
369 steatosis.[38] Interestingly, the consumption of TAN effectively reduced the hepatic
370 accumulation of FFAs, DGs, CERs, and TGs ($p < 0.05$), suggesting that TAN could
371 improve hepatic steatosis. However, the metabolisms of TGs, DGs and FFAs are closely
372 related to the genes participated in lipogenesis (*SREBP-1c*, *ACC* and *FAS*) and lipid
373 oxidation (*AMPK*, *PPAR-α* and *CPT1*). *SREBP-1c*, *ACC* and *FAS* are considered to be
374 important regulators of lipogenic genes, which are closely linked with an increment of
375 de novo lipogenesis.[39] *SREBP-1c* is an important transcription factor in lipogenesis via
376 mediating the expression of downstream genes *ACC* and *FAS*, which regulate TG and
377 fatty acids synthesis.[34,40] In this study, the consumption of TAN suppressed the
378 expression levels of genes *SREBP-1c*, *ACC* and *FAS* to inhibit TGs formation and fatty

379 acid biosynthesis, thereby contributing to the decline of the total content of TGs, DGs
380 and FFAs in lipidomic profiles and the lower levels of hepatic TG (Figure 8B).
381 Moreover, TAN treatment elevated the *AMPK* mRNA level and its downstream gene
382 *CPT1* level. The activation of *AMPK* in the liver induced *PPAR-α* and *CPT1* production,
383 which can accelerate fatty acid oxidation.[41] On the other hand, the decline in FFAs
384 content was closely related to the up-regulation of *AMPK* and *CPT1* by TAN treatment
385 (Figure 8B). In addition, stearoyl-CoA desaturase (*SCD1*) have been proved to be
386 closely associated with increasing lipogenesis and the synthesis of CEs.[42] SCD-1-
387 deficient mice showed a lowering levels of CEs.[43] In the present study, TAN
388 supplementation not only significantly inhibited the expression of gene *SCD1* but also
389 upregulated the mRNA expression of *CYP7A1* and *CYP27A1*, which stimulate
390 cholesterol conversion to bile acids, thereby reducing the total content of CEs in liver
391 and hepatic TC level (Figure 8B). Hence, these results suggested that TAN might exert
392 a cholesterol-lowering effect on rats induced by an HFD.

393 The remarkable increment in DG species are a hallmark of NAFLD.[44] An increase
394 of oleate-containing DGs was observed in obesity, and hepatic monounsaturated DGs
395 were elevated and correlated with HOMA-IR, while human carboxylesterase 2 reversed
396 obesity-induced diacylglycerol accumulation in humans.[45] DGs are known to regulate
397 insulin resistance by the activation of protein kinase C and then suppress its intrinsic
398 tyrosine kinase activity in nonalcoholic fatty liver disease.[46] Furthermore, previous
399 studies also demonstrated that TAN could enhance insulin resistance.[30] Similar to

previous results, an increase of DGs, including most of oleic acid-containing DGs were observed on rats induced by an HFD in this study. Whereas TAN dramatically decreased the hepatic accumulation of five oleate-containing DGs, such as DG (18:1/20:3), DG (18:4/18:1), DG (18:1/22:4), DG (18:1/20:5), and DG (18:1/22:5). Therefore, these five oleate-containing DGs might be strongly correlated with the anti-obesity and lipid-lowering effects of TAN. Further study is required to verify the signaling mechanisms. Additionally, the changes in the relative abundance of PEs and impairment of PE metabolism would disorder hepatic function via multiple mechanisms, especially in hepatic steatosis.[47] An increase of PEs promotes coalescence between lipid droplets and then increases lipid droplet size.[48] When contrasted with the HFD group, the relative intensities of three PEs (PE (14:0/18:1), PE (18:1/18:0), and PE (18:1/18:1)) were dramatically reduced in HFD+HTAN group, which might be related to improve hepatic steatosis due to prevent coalescence of the lipid droplets.

In summary, we demonstrated that supplementation of TAN could prevent obesity, dyslipidemia and hepatic steatosis resulting from the dysregulation of lipid metabolism. These beneficial effects were associated with the lowering of FFAs, DGs, TGs, CERs and CEs in the liver as indicated by lipidomics analysis. Lipidomics profiling has proved helpful to strengthen our understanding of bioactivities of functional foods, and might provide new insights into the interactions between functional foods and lipid metabolism.

ASSOCIATED CONTENT

Supporting information

Table S1. The origins of tangerine peel oil samples.

Table S2. Composition and energy distribution of animal diets.

Table S3. Primer sequences used for qRT-PCR.

Supplementary file 1. Lipidomics analysis of lipid abundance in liver samples.

Supplementary file 2. Heatmap for hierarchical cluster analysis of lipid profiles in liver among three groups.

AUTHOR INFORMATION

Corresponding authors

Yong Cao, Fax (Tel.): +86(020)8586234, E-mail: caoyong2181@scau.edu.cn.

Yunjiao Chen, Fax (Tel.): +86(020)8586234, E-mail: yunjiaochen@scau.edu.cn.

Funding

This work was financially supported by National Key R&D Program of China-Technological innovation of artificial forest non-wood forest resources High-quality utilization (2016YFD0600806), Guangdong Provincial Key Laboratory of Nutraceuticals and Functional Foods (2018B030322010) and the Program for Guangdong Introducing Innovative and Entrepreneurial Teams (2019ZT08N291).

Notes

The authors declare no competing financial interest.

ABBREVIATIONS USED

ACC, acetyl-CoA carboxylase; ALT, alanine aminotransferase; *AMPK*, 5′ AMP-activated protein kinase; AST, aspartate aminotransferase; *CPT1*, carnitine palmitoyltransferase 1; *FAS*, fatty acid synthase; HDL-C, high-density lipoprotein cholesterol; HFD, high-fat diet; HMF, heptamethoxyflavone; LDL-C, low density lipoprotein cholesterol; ND, normal diet; NOB, nobiletin; *PPARα*, peroxisome proliferator-activated receptor α; *PPARγ*, peroxisome proliferator-activated receptor γ; *SCD1*, stearoyl-CoA desaturase; *SREBP-1c*, sterol regulatory element-binding protein-1c; TC, total cholesterol; TG, triacylglycerol; TPO, tangerine peel oil.

REFERENCES

(1). Gao, Z.; Gao, W.; Zeng, S.-L.; Li, P.; Liu, E. H., Chemical structures, bioactivities and molecular mechanisms of citrus polymethoxyflavones. *J. Funct. Foods* **2018,** *40*, 498-509.

(2). Ting, Y.; Chiou, Y. S.; Jiang, Y.; Pan, M. H.; Lin, Z.; Huang, Q., Safety evaluation of tangeretin and the effect of using emulsion-based delivery system: Oral acute and 28-day sub-acute toxicity study using mice. *Food Res. Int.* **2015,** *74*, 140-150.

(3). Miyata, Y.; Tanaka, H.; Shimada, A.; Sato, T.; Ito, A.; Yamanouchi, T.; Kosano, H., Regulation of adipocytokine secretion and adipocyte hypertrophy by polymethoxyflavonoids, nobiletin and tangeretin. *Life Sci.* **2011,** *88* (13-14), 613-618.

463 (4). Kim, M. S.; Hur, H. J.; Kwon, D. Y.; Hwang, J. T., Tangeretin stimulates glucose
464 uptake via regulation of AMPK signaling pathways in C2C12 myotubes and improves
465 glucose tolerance in high-fat diet-induced obese mice. *Mol. Cell. Endocrinol.* **2012,** *358*
466 (1), 127-134.
467 (5). Omar, H. A.; Mohamed, W. R.; Arab, H. H.; Arafa el, S. A., Tangeretin alleviates
468 cisplatin-induced acute hepatic injury in rats: Targeting MAPKs and apoptosis. *PLoS*
469 *One* **2016,** *11* (3), e0151649.
470 (6). Liang, F.; Fang, Y.; Cao, W.; Zhang, Z.; Pan, S.; Xu, X., Attenuation of tert-butyl
471 hydroperoxide (t-BHP)-induced oxidative damage in HepG2 cells by tangeretin:
472 Relevance of the Nrf2–ARE and MAPK signaling pathways. *J. Agric. Food Chem.*
473 **2018,** *66* (25), 6317-6325.
474 (7). Lee, Y. Y.; Lee, E. J.; Park, J. S.; Jang, S. E.; Kim, D. H.; Kim, H. S., Anti-
475 Inflammatory and antioxidant mechanism of tangeretin in activated microglia. *J.*
476 *Neuroimmune Pharmacol.* **2016,** *11* (2), 294-305.
477 (8). Mulvihill, E. E.; Burke, A. C.; Huff, M. W., Citrus flavonoids as regulators of
478 lipoprotein metabolism and atherosclerosis *Annu. Rev. Nutr.* **2016,** *36*, 275-299.
479 (9). Zeng, S. L.; Li, S. Z.; Xiao, P. T.; Cai, Y. Y.; Chu, C.; Chen, B. Z.; Li, P.; Li, J.; Liu,
480 E. H., Citrus polymethoxyflavones attenuate metabolic syndrome by regulating gut
481 microbiome and amino acid metabolism. *Sci. Adv.* **2020,** *6* (1), eaax6208.
482 (10). Kurowska, E. M.; Manthey, J. A.; Casaschi, A.; Theriault, A. G., Modulation of
483 hepG2 cell net apolipoprotein B secretion by the citrus polymethoxyflavone, tangeretin.

Lipids **2004,** *39* (2), 143-151.

(11). Kurowska, E. M.; Manthey, J. A., Hypolipidemic effects and absorption of citrus polymethoxylated flavones in hamsters with diet-induced hypercholesterolemia. *J. Agric. Food Chem.* **2004,** *52* (10), 2879-2886.

(12). Tung, Y.-C.; Chang, W.-T.; Li, S.; Wu, J.-C.; Badmeav, V.; Ho, C.-T.; Pan, M.-H., Citrus peel extracts attenuated obesity and modulated gut microbiota in a high-fat diet-induced obesity mice. *Food Funct.* **2018,** *9* (6), 3363-3373.

(13). Assini, J. M.; Mulvihill, E. E.; Huff, M. W., Citrus flavonoids and lipid metabolism. *Curr. Opin. Lipidol.* **2013,** *24* (1), 34-40.

(14). Yang, K.; Han, X., Lipidomics: techniques, applications, and outcomes related to biomedical sciences. *Trends Biochem. Sci.* **2016,** *41* (11), 954-969.

(15). Han, X.; Gross, R. W., Global analyses of cellular lipidomes directly from crude extracts of biological samples by ESI mass spectrometry: A bridge to lipidomics. *J. Lipid Res.* **2010,** *44* (6), 1071-1079.

(16). Han, X., Lipidomics for studying metabolism. *Nat. Rev. Endocrinol.* **2016,** *12* (11), 668-679.

(17). Ibanez, C.; Mouhid, L.; Reglero, G.; Ramirez de Molina, A., Lipidomics insights in health and nutritional intervention studies. *J. Agric. Food Chem.* **2017,** *65* (36), 7827-7842.

(18). Nie, Q.; Xing, M.; Chen, H.; Hu, J.; Nie, S., Metabolomics and lipidomics profiling reveals hypocholesterolemic and hypolipidemic effects of arabinoxylan on

505 Type 2 diabetic rats. *J. Agric. Food Chem.* **2019,** *67* (38), 10614-10623.

506 (19). Wen, J. J.; Gao, H.; Hu, J. L.; Nie, Q. X.; Chen, H. H.; Xiong, T.; Nie, S. P.; Xie,

507 M. Y., Polysaccharides from fermented *Momordica charantia* ameliorate obesity in

508 high-fat induced obese rats. *Food Funct.* **2019,** *10* (1), 448-457.

509 (20). Maskrey, B. H.; Megson, I. L.; Rossi, A. G.; Whitfield, P. D., Emerging

510 importance of omega-3 fatty acids in the innate immune response: Molecular

511 mechanisms and lipidomic strategies for their analysis. *Mol. Nutr. Food Res.* **2013,** *57*

512 (8), 1390-1400.

513 (21). Feng, K.; Zhu, X.; Chen, T.; Peng, B.; Lu, M.; Zheng, H.; Huang, Q.; Ho, C. T.;

514 Chen, Y.; Cao, Y., Prevention of obesity and hyperlipidemia by heptamethoxyflavone

515 in high-fat diet-induced rats. *J. Agric. Food Chem.* **2019,** *67* (9), 2476-2489.

516 (22). Tung, Y. C.; Li, S.; Huang, Q.; Hung, W. L.; Ho, C. T.; Wei, G. J.; Pan, M. H., 5-

517 Demethylnobiletin and 5-acetoxy-6,7,8,3',4'-pentamethoxyflavone suppress lipid

518 accumulation by activating the LKB1-AMPK pathway in 3T3-L1 preadipocytes and

519 high fat diet-fed C57BL/6 mice. *J. Agric. Food Chem.* **2016,** *64* (16), 3196-205.

520 (23). Zhang, M.; Zhu, J.; Zhang, X.; Zhao, D.; Ma, Y.; Li, D.; Ho, C.-T.; Huang, Q.,

521 Aged citrus peel (chenpi) extract causes dynamic alteration of colonic microbiota in

522 high-fat diet induced obese mice. *Food Funct.* **2020**.

523 (24). Zhao, L.; Zhang, Y.; He, L.; Dai, W.; Lai, Y.; Yao, X.; Cao, Y., Soy sauce residue

524 oil extracted by a novel continuous phase transition extraction under low temperature

525 and its refining process. *J. Agric. Food Chem.* **2014,** *62* (14), 3230-3235.

526 (25). Feng, S.; Gan, L.; Yang, C. S.; Liu, A. B.; Lu, W.; Shao, P.; Dai, Z.; Sun, P.; Luo,
527 Z., Effects of stigmasterol and beta-sitosterol on nonalcoholic fatty liver disease in a
528 mouse model: A lipidomic analysis. *J. Agric. Food Chem.* **2018,** *66* (13), 3417-3425.
529 (26). Wang, F.; Chen, L.; Chen, H.; Chen, S.; Liu, Y., Analysis of flavonoid metabolites
530 in citrus peels (Citrus reticulata "*Dahongpao*") using UPLC-ESI-MS/MS. *Molecules*
531 **2019,** *24* (15), 2680.
532 (27). Zhu, X.; Qiu, Z.; Ouyang, W.; Miao, J.; Xiong, P.; Mao, D.; Feng, K.; Li, M.; Luo,
533 M.; Xiao, H.; Cao, Y., Hepatic transcriptome and proteome analyses provide new
534 insights into the regulator mechanism of dietary avicularin in diabetic mice. *Food Res.*
535 *Int.* **2019,** *125*, 108570.
536 (28). Kumar, S.; Pandey, A. K., Chemistry and biological activities of flavonoids: An
537 overview. *Sci. World J.* **2013,** *2013*, 1-16.
538 (29). Gao, Z.; Gao, W.; Zeng, S. L.; Li, P.; Liu, E. H., Chemical structures, bioactivities
539 and molecular mechanisms of citrus polymethoxyflavones. *J. Funct. Foods* **2018,** *40*,
540 498-509.
541 (30). Sundaram, R.; Shanthi, P.; Sachdanandam, P., Tangeretin, a polymethoxylated
542 flavone, modulates lipid homeostasis and decreases oxidative stress by inhibiting NF-
543 κB activation and proinflammatory cytokines in cardiac tissue of streptozotocin-
544 induced diabetic rats. *J. Funct. Foods* **2015,** *16*, 315-333.
545 (31). Lee, Y. S.; Cha, B. Y.; Choi, S. S.; Choi, B. K.; Yonezawa, T.; Teruya, T.; Nagai,
546 K.; Woo, J. T., Nobiletin improves obesity and insulin resistance in high-fat diet-

547 induced obese mice. *J. Nutr. Biochem.* **2013,** *24* (1), 156-162.

548 (32). Guo, J.; Tao, H.; Cao, Y.; Ho, C. T.; Jin, S.; Huang, Q., Prevention of obesity and
549 type 2 diabetes with aged citrus peel (Chenpi) extract. *J. Agric. Food Chem.* **2016,** *64*
550 (10), 2053-2061.

551 (33). Lai, C. S.; Ho, M. H.; Tsai, M. L.; Li, S.; Badmaev, V.; Ho, C. T.; Pan, M. H.,
552 Suppression of adipogenesis and obesity in high-fat induced mouse model by
553 hydroxylated polymethoxyflavones. *J. Agric. Food Chem.* **2013,** *61* (43), 10320-10328.

554 (34). Wang, L.; Li, C.; Huang, Q.; Fu, X., Polysaccharide from Rosa roxburghii Tratt
555 fruit attenuates hyperglycemia and hyperlipidemia and regulates colon microbiota in
556 diabetic db/db mice. *J. Agric. Food Chem.* **2020,** *68* (1), 147-159.

557 (35). Preuss, C.; Jelenik, T.; Bodis, K.; Mussig, K.; Burkart, V.; Szendroedi, J.; Roden,
558 M.; Markgraf, D. F., A new targeted lipidomics approach reveals lipid droplets in liver,
559 muscle and heart as a repository for diacylglycerol and ceramide species in non-
560 alcoholic fatty liver. *Cells* **2019,** *8* (3).

561 (36). Yang, Y.; Sun, Q.; Xu, X.; Yang, X.; Gao, Y.; Sun, X.; Zhao, Y.; Ding, Z.; Ge, W.;
562 Cheng, R.; Zhang, J., Oral Administration of succinoglycan riclin improves diet-
563 induced hypercholesterolemia in mice. *J. Agric. Food Chem.* **2019,** *67* (48), 13307-
564 13317.

565 (37). Feng, S.; Dai, Z.; Liu, A. B.; Huang, J.; Narsipur, N.; Guo, G.; Kong, B.; Reuhl,
566 K.; Lu, W.; Luo, Z.; Yang, C. S., Intake of stigmasterol and beta-sitosterol alters lipid
567 metabolism and alleviates NAFLD in mice fed a high-fat western-style diet. *Biochim.*

568 *Biophys. Acta, Mol. Cell Biol. Lipids* **2018,** *1863* (10), 1274-1284.

569 (38). Neuschwander‐Tetri, B. A., Hepatic lipotoxicity and the pathogenesis of
570 nonalcoholic steatohepatitis: The central role of nontriglyceride fatty acid metabolites.
571 *Hepatology* **2010,** *52* (2), 774-788.

572 (39). Chirala, S. S.; Chang, H. M.; Abu, E. L.; Mao, J.; Mahon, K.; Finegold, M.; Wakil,
573 S. J., Fatty acid synthesis is essential in embryonic development: fatty acid synthase
574 null mutants and most of the heterozygotes die in utero. *Proc. Natl. Acad. Sci.* **2003,**
575 *100* (11), 6358-6363.

576 (40). Rosen, E. D.; Walkey, C. J.; Puigserver, P.; Spiegelman, B. M., Transcriptional
577 regulation of adipogenesis. *Genes Dev.* **2000,** *14* (11), 1293-1307.

578 (41). Tung, Y. T.; Chen, H. L.; Wu, H. S.; Ho, M. H.; Chong, K. Y.; Chen, C. M., Kefir
579 peptides prevent hyperlipidemia and obesity in high-fat-diet-induced obese rats via
580 lipid metabolism modulation. *Mol. Nutr. Food Res.* **2018,** *62* (3), 1700505.

581 (42). Paton, C. M.; Ntambi, J. M., Biochemical and physiological function of stearoyl-
582 CoA desaturase. *Am. J. Physiol.: Endocrinol. Metab.* **2009,** *297* (1), E28-E37.

583 (43). Miyazaki, M.; Kim, Y.-C.; Gray-Keller, M. P.; Attie, A. D.; Ntambi, J. M., The
584 biosynthesis of hepatic cholesterol esters and triglycerides is impaired in mice with a
585 disruption of the gene for stearoyl-CoA desaturase 1. *J. Biol. Chem.* **2000,** *275* (39),
586 30132-30138.

587 (44). Gorden, D. L.; Ivanova, P. T.; Myers, D. S.; McIntyre, J. O.; VanSaun, M. N.;
588 Wright, J. K.; Matrisian, L. M.; Brown, H. A., Increased diacylglycerols characterize

589 hepatic lipid changes in progression of human nonalcoholic fatty liver disease;
590 comparison to a murine model. *PLoS One* **2011,** *6* (8), e22775.
591 (45). Ruby, M. A.; Massart, J.; Hunerdosse, D. M.; Schönke, M.; Correia, J. C.; Louie,
592 S. M.; Ruas, J. L.; Näslund, E.; Nomura, D. K.; Zierath, J. R., Human carboxylesterase
593 2 reverses obesity-induced diacylglycerol accumulation and glucose intolerance. *Cell*
594 *Rep.* **2017,** *18* (3), 636-646.
595 (46). Dries, D. R.; Gallegos, L. L.; Newton, A. C., A Single residue in the c1 domain
596 sensitizes novel protein kinase c isoforms to cellular diacylglycerol production. *J. Biol.*
597 *Chem.* **2007,** *282* (2), 826-830.
598 (47). Calzada, E.; Onguka, O.; Claypool, S. M., phosphatidylethanolamine metabolism
599 in health and disease. *Int. Rev. Cell Mol. Biol.* **2016,** *321*, 29-88.
600 (48). Cohen, B.-C.; Raz, C.; Shamay, A.; Argov-Argaman, N., Lipid droplet fusion in
601 mammary epithelial cells is regulated by phosphatidylethanolamine metabolism. *J.*
602 *Mammary Gland Biol.* **2017,** *22* (4), 235-249.
603
604
605
606
607
608
609

610 **Figure Legend**

611 **Figure 1.** Separation and purification of NOB and TAN. The content of major PMFs
612 from 22 tangerine peel oil samples in different origins (A). The procedures of
613 simultaneous separation and purification of NOB and TAN (B). The chemical structure
614 of tangeretin (C). HPLC chromatograph of PMFs from TPO sample 19 (D) and the
615 white crystal of TAN (E). Peak 1, NOB; Peak 2, HMF, Peak 3, TAN.

616

617 **Figure 2.** Effects of TAN supplement on serum TC (A), TG (B), HDL-C (C), LDL-C
618 (D), ALT (E), and AST (F) concentrations. The ND and HFD groups for serum
619 biochemistry in rats were to previously published data.[21] Data are presented as mean ±
620 SD (n = 8). Multiple comparison among groups was carried out by using Duncan's
621 multiple range test in ANOVA analysis. Mean values with different letters represent
622 statistically significant differences ($p < 0.05$). ND: normal diet group, HFD: high-fat
623 diet group, HFD+LTAN: high-fat diet with 0.02% TAN group, HFD+MTAN: high-fat
624 diet with 0.04% TAN group, HFD+HTAN: high-fat diet with 0.08% TAN group.

625

626 **Figure 3.** Effect of TAN supplement on the hepatic TC levels (A), hepatic TG levels
627 (B), liver samples (C), and representative H&E-stained images of the liver (D)
628 (magnification, 100× and 400×). Data are presented as mean ± SD (n = 8).

629

630 **Figure 4.** Lipidomics analysis of liver samples. The intensity of different lipid

631 compositions in the liver (A, B and C). Principal component analysis (PCA) score plots
632 of hepatic lipid profiling among all groups (D). Data are presented as mean ± SD (n =
633 4). Different letters indicate statistically significant differences ($p < 0.05$). TG:
634 triacylglycerol, PC: phosphatidylcholine, SM: sphingomyelins, LPC:
635 lysophosphatidylcholine, PE: phosphatidylethanolamine, LPE:
636 lysophosphatidylethanolamine, DG: diacylglycerol, CER: ceramide, FFA: free fatty
637 acids, CE: cholesteryl esters, CAR: carnitine, PS: phosphatidylserine, COQ: Coenzyme
638 Q, PI: phosphatidylinositol, MG: monoacylglycerol, PG: phosphatidylglycerol, LPS:
639 lysophosphatidylserine, PA: phosphatidic acid, LPI: lysophosphatidylinositol, LPG:
640 lysophosphatidylglycerol.
641
642 **Figure 5.** Analysis of significantly differential lipid species in ND versus HFD and
643 HFD versus HFD+HTAN. OPLS-DA scores plots (A, B) and volcano plot (C, D)
644 analysis of ND versus HFD and HFD versus HFD+HTAN, respectively. The potential
645 lipid biomarkers responsible for anti-obesity and cholesterol-lowering effects of TAN
646 (E and F). A number of significantly differential lipid species were selected out by using
647 the criteria of a FC $\geqslant$ 2 or $\leqslant$ 0.5 and VIP $\geqslant$ 1 in the volcano plot. Significantly
648 differential lipid species were shown as a red (up) or green (down) dot, whereas a gray
649 dot represented no significant difference of lipid species. Data are presented as mean ±
650 SD (n = 4).
651

652 **Figure 6.** Heatmap of significantly differential lipid species in ND versus HFD. Colors
653 represent the contents of different lipid classes with red meaning a high content of lipids
654 and green meaning a low content.
655
656 **Figure 7.** Lipid metabolic pathway analysis based on significantly differential lipid
657 species in ND versus HFD (A) and HFD versus HFD+HTAN (B). Degree of enrichment
658 was analyzed by a rich factor, P-value and the number of lipid metabolites that enriched
659 in each pathway. The size of bubble means the amount of significantly differential lipid
660 species which are enriched in this pathway, and the point with different gradation of
661 color represents the scope of P-value. The higher value of rich factor stands for the
662 higher degree of enrichment, and the lower P-value represents the more significant
663 degree of enrichment.
664
665 **Figure 8.** Effects of TAN supplement on the expression levels of hepatic lipid
666 metabolism genes (A). Data are presented as means ± SD (n = 6). The relative mRNA
667 expression levels of genes were analyzed referring to the $2^{-\Delta\Delta C}{}_T$ method and normalized
668 to the GAPDH gene. Possible mechanisms of TAN supplementation for suppression of
669 obesity, hypercholesterolemia and hepatic steatosis in rats induced by an HFD (B).
670 Briefly, TAN supplementation could regulate the lipid metabolism through
671 downregulating the expression levels of genes *SREBP-1c*, *ACC*, *SCD1* and *FAS* so as
672 to inhibit fatty acids and TG synthesis and upregulating the expression of genes *AMPK*

673 and *CPT1* leading to increase lipid oxidation, as well as upregulating the expression of
674 genes *CYP7A1* and *CYP27A1*so as to increase bile acid biosynthesis. Subsequently, the
675 decline of hepatic accumulation of FFAs, DGs, CERs, TGs and CEs resulted in the
676 reduction of lipid accumulation, thereby contributing to lowering body weight, body
677 fat, hepatic TC and TG levels and serum TC and LDL-C levels.
678
679
680
681
682

Figure 1

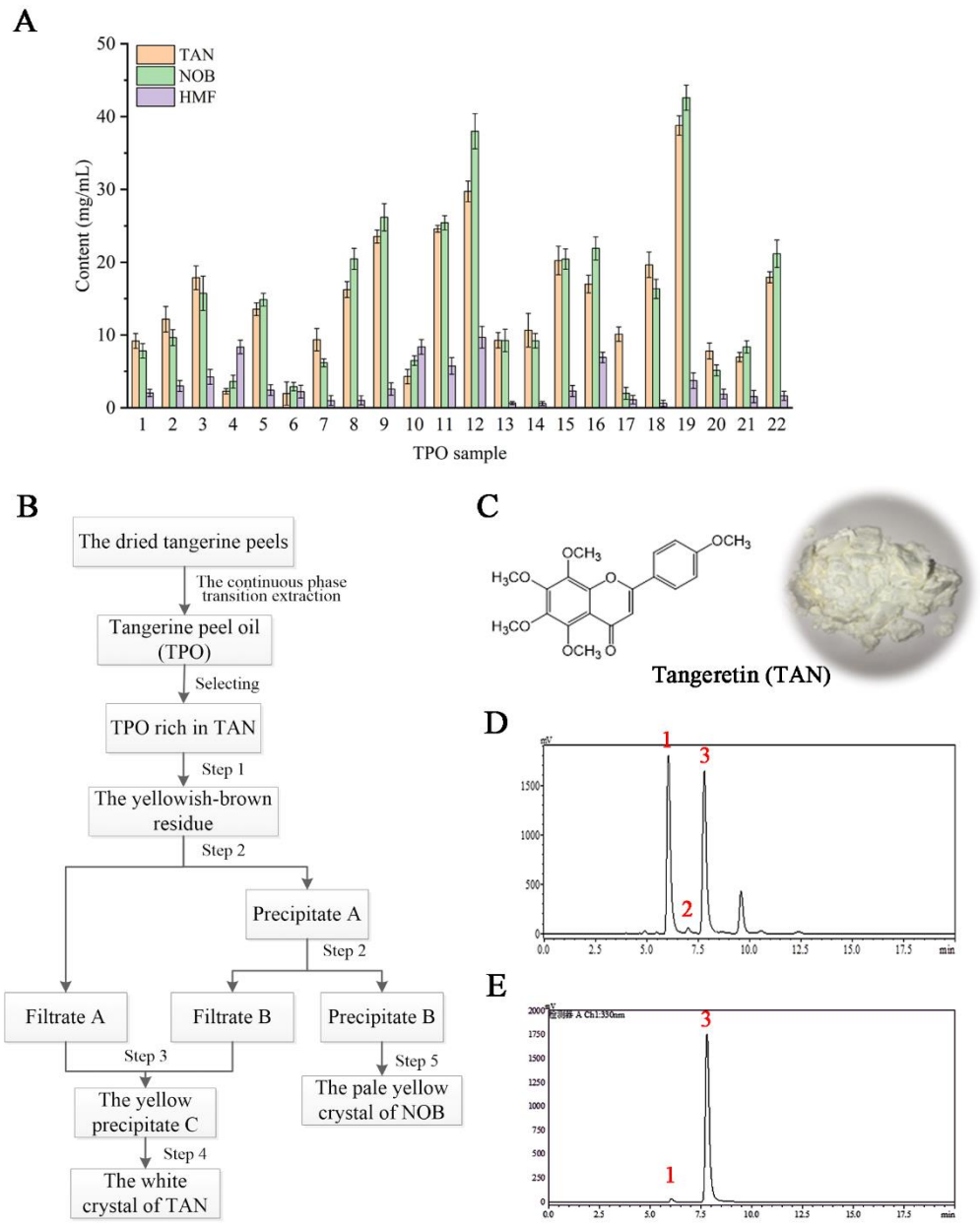
A
TAN
NOB
HMF
Content (mg/mL)
TPO sample
B
The dried tangerine peels
The continuous phase transition extraction
Tangerine peel oil (TPO)
Selecting
TPO rich in TAN
Step 1
The yellowish-brown residue
Step 2
Precipitate A
Step 2
Filtrate A
Filtrate B
Precipitate B
Step 3
Step 5
The yellow precipitate C
The pale yellow crystal of NOB
Step 4
The white crystal of TAN
C
Tangeretin (TAN)
D
E

Figure 2

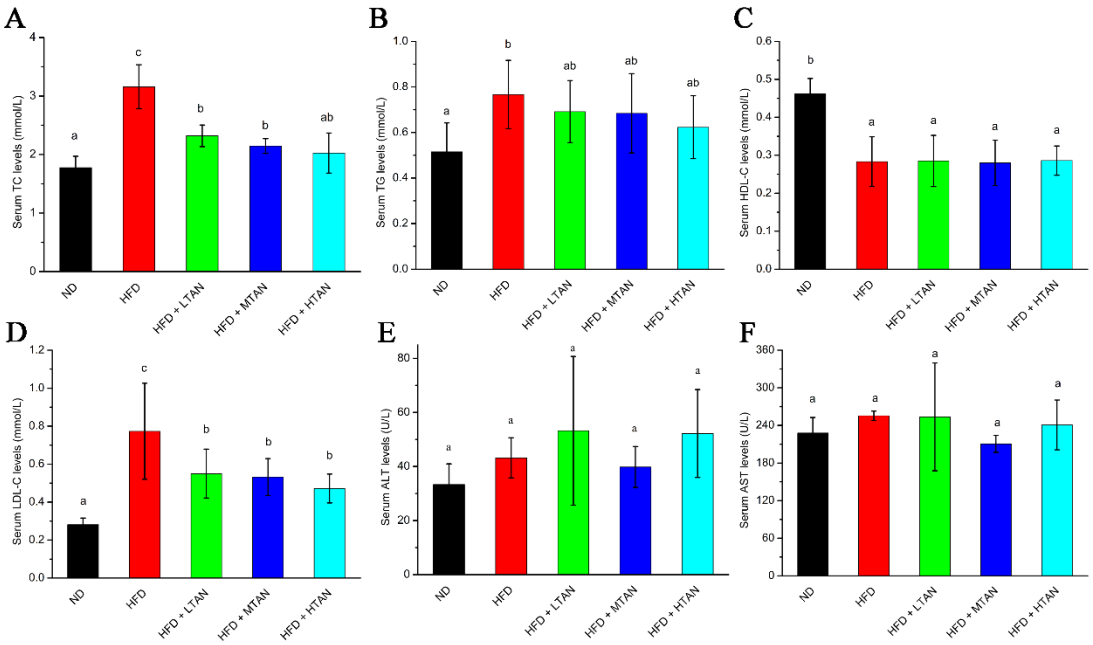
A
Serum TC levels (mmol/L)
B
Serum TG levels (mmol/L)
C
Serum HDL-C levels (mmol/L)
D
Serum LDL-C levels (mmol/L)
E
Serum ALT levels (U/L)
F
Serum AST levels (U/L)
ND
HFD
HFD + LTAN
HFD + MTAN
HFD + HTAN

Figure 3

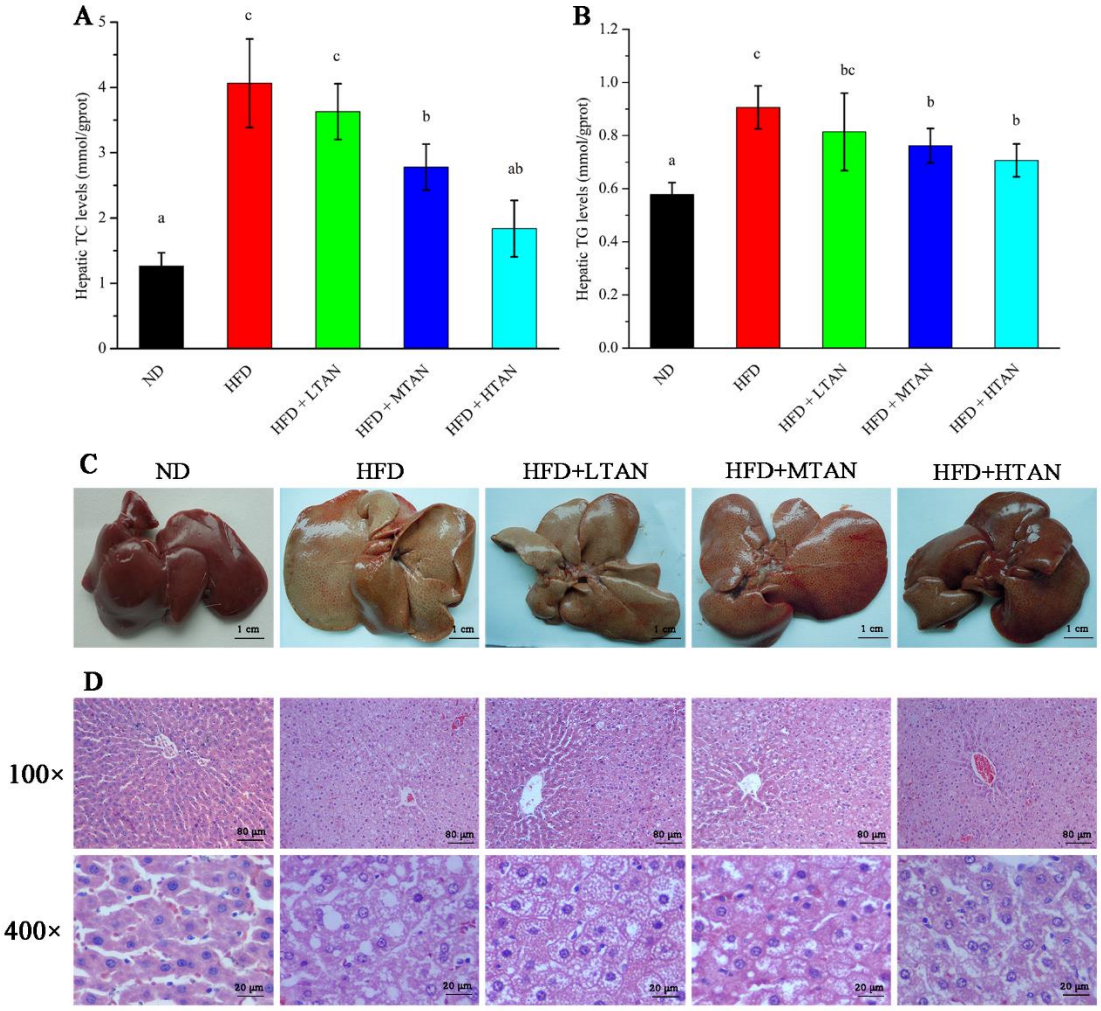
A
Hepatic TC levels (mmol/gprot)
a
c
c
b
ab
ND
HFD
HFD + LTAN
HFD + MTAN
HFD + HTAN
B
Hepatic TG levels (mmol/gprot)
a
c
bc
b
b
C
ND
HFD
HFD+LTAN
HFD+MTAN
HFD+HTAN
1 cm
D
100×
400×
80 μm
20 μm

Figure 4

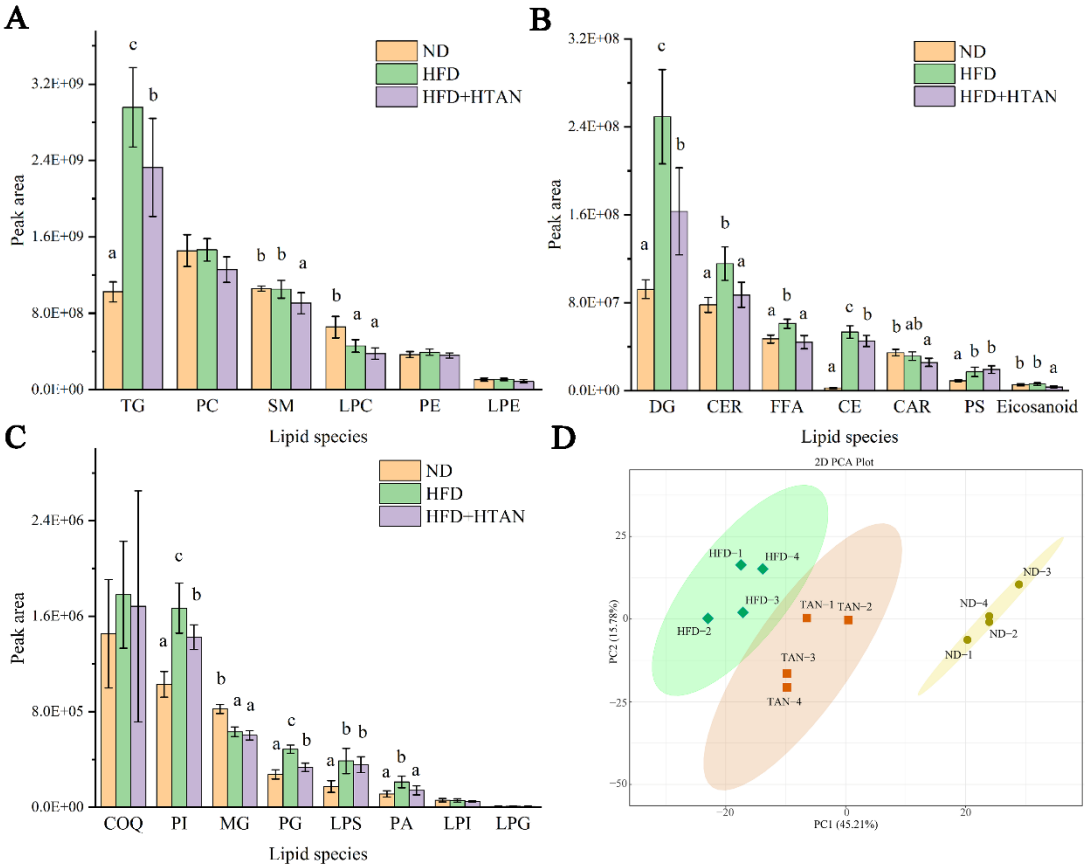
A
ND
HFD
HFD+HTAN
Peak area
3.2E+09
2.4E+09
1.6E+09
8.0E+08
0.0E+00
TG
PC
SM
LPC
PE
LPE
Lipid species
B
ND
HFD
HFD+HTAN
Peak area
3.2E+08
2.4E+08
1.6E+08
8.0E+07
0.0E+00
DG
CER
FFA
CE
CAR
PS
Eicosanoid
Lipid species
C
ND
HFD
HFD−HTAN
Peak area
2.4E+06
1.6E+06
8.0E+05
0.0E+00
COQ
PI
MG
PG
LPS
PA
LPI
LPG
Lipid species
D
2D PCA Plot
PC2 (15.78%)
PC1 (45.21%)
HFD−1
HFD−4
HFD−3
HFD−2
TAN−1
TAN−2
TAN−3
TAN−4
ND−3
ND−4
ND−2
ND−1

Figure 5

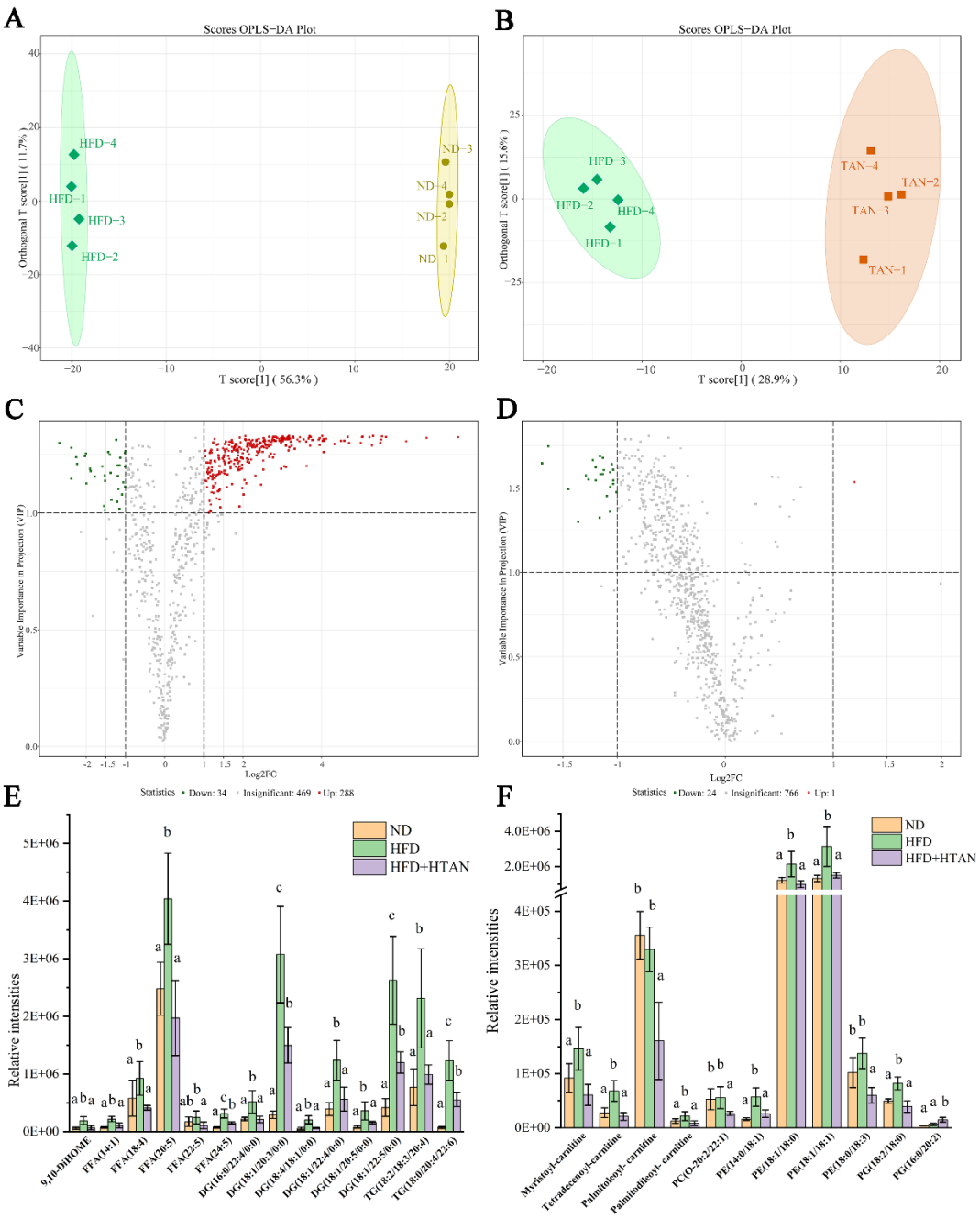
A
Scores OPLS-DA Plot
Orthogonal T score[1] (11.7%)
T score[1] (56.3%)
HFD-4
HFD-1
HFD-3
HFD-2
ND-3
ND-4
ND-2
ND-1
B
Scores OPLS-DA Plot
Orthogonal T score[1] (15.6%)
T score[1] (28.9%)
HFD-3
HFD-2
HFD-4
HFD-1
TAN-4
TAN-2
TAN-3
TAN-1
C
Variable Importance in Projection (VIP)
Log2FC
Statistics • Down: 34 • Insignificant: 469 • Up: 288
D
Variable Importance in Projection (VIP)
Log2FC
Statistics • Down: 24 • Insignificant: 766 • Up: 1
E
Relative intensities
ND
HFD
HFD+HTAN
9,10-DHOME
FFA(14:1)
FFA(18:4)
FFA(20:5)
FFA(22:5)
FFA(24:5)
DG(16:0/22:4/0:0)
DG(18:1/20:3/0:0)
DG(18:4/18:1/0:0)
DG(18:1/22:4/0:0)
DG(18:1/20:5/0:0)
DG(18:1/22:5/0:0)
TG(18:2/18:3/20:4)
TG(18:0/20:4/22:6)
F
Relative intensities
ND
HFD
HFD+HTAN
Myristoyl-carnitine
Tetradecenoyl-carnitine
Palmitoleoyl- carnitine
Palmitodienoyl- carnitine
PC(O-20:2/22:1)
PE(14:0/18:1)
PE(18:1/18:0)
PE(18:1/18:1)
PE(18:0/18:3)
PG(18:2/18:0)
PG(16:0/20:2)

Figure 6

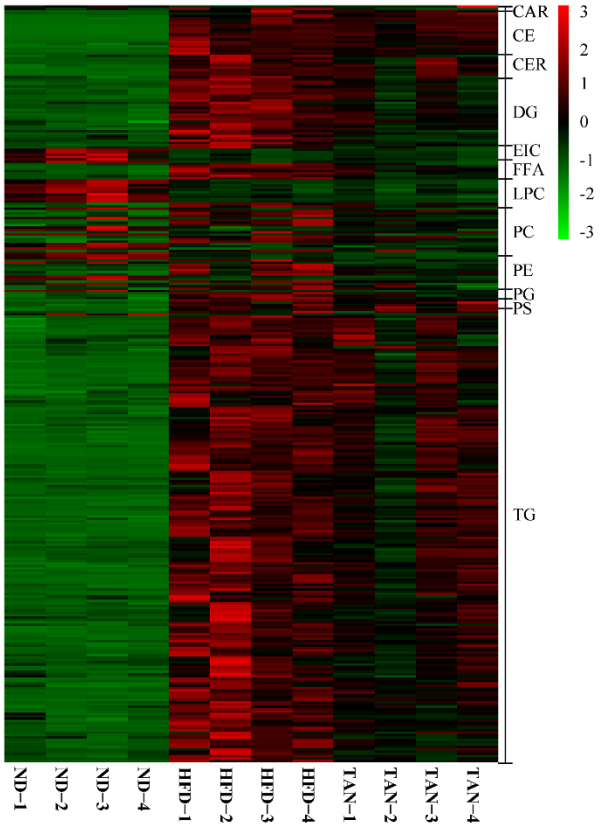
CAR
CE
CER
DG
EIC
FFA
LPC
PC
PE
PG
PS
TG
3
2
1
0
-1
-2
-3
ND−1
ND−2
ND−3
ND−4
HFD−1
HFD−2
HFD−3
HFD−4
TAN−1
TAN−2
TAN−3
TAN−4

Figure 7

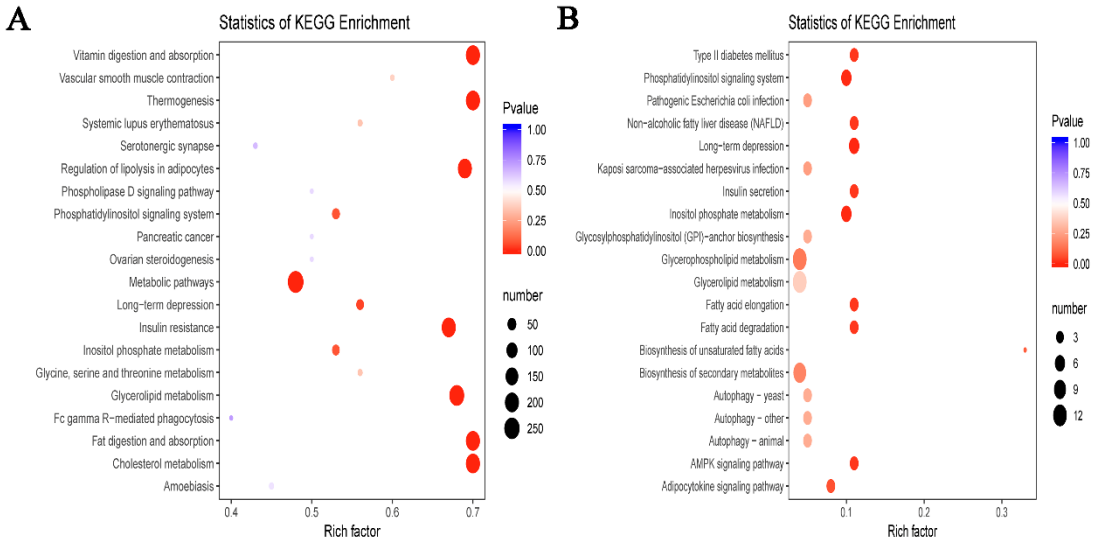
A
Statistics of KEGG Enrichment
Vitamin digestion and absorption
Vascular smooth muscle contraction
Thermogenesis
Systemic lupus erythematosus
Serotonergic synapse
Regulation of lipolysis in adipocytes
Phospholipase D signaling pathway
Phosphatidylinositol signaling system
Pancreatic cancer
Ovarian steroidogenesis
Metabolic pathways
Long−term depression
Insulin resistance
Inositol phosphate metabolism
Glycine, serine and threonine metabolism
Glycerolipid metabolism
Fc gamma R−mediated phagocytosis
Fat digestion and absorption
Cholesterol metabolism
Amoebiasis
0.4
0.5
0.6
0.7
Rich factor
Pvalue
1.00
0.75
0.50
0.25
0.00
number
50
100
150
200
250
B
Statistics of KEGG Enrichment
Type II diabetes mellitus
Phosphatidylinositol signaling system
Pathogenic Escherichia coli infection
Non−alcoholic fatty liver disease (NAFLD)
Long−term depression
Kaposi sarcoma−associated herpesvirus infection
Insulin secretion
Inositol phosphate metabolism
Glycosylphosphatidylinositol (GPI)−anchor biosynthesis
Glycerophospholipid metabolism
Glycerolipid metabolism
Fatty acid elongation
Fatty acid degradation
Biosynthesis of unsaturated fatty acids
Biosynthesis of secondary metabolites
Autophagy − yeast
Autophagy − other
Autophagy − animal
AMPK signaling pathway
Adipocytokine signaling pathway
0.1
0.2
0.3
Rich factor
Pvalue
1.00
0.75
0.50
0.25
0.00
number
3
6
9
12

Figure 8

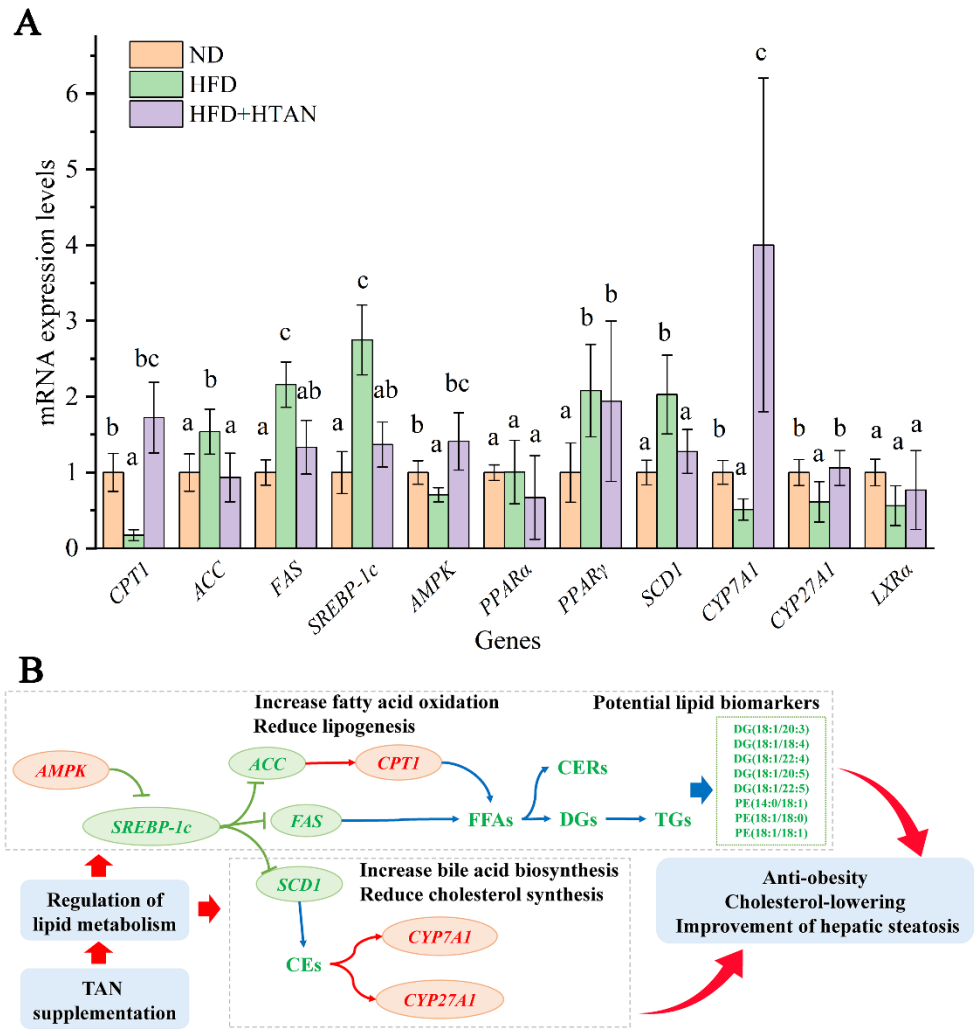
A
ND
HFD
HFD+HTAN
mRNA expression levels
Genes
CPT1
ACC
FAS
SREBP-1c
AMPK
PPARα
PPARγ
SCD1
CYP7A1
CYP27A1
LXRα
B
Increase fatty acid oxidation
Reduce lipogenesis
Potential lipid biomarkers
DG(18:1/20:3)
DG(18:1/18:4)
DG(18:1/22:4)
DG(18:1/20:5)
DG(18:1/22:5)
PE(14:0/18:1)
PE(18:1/18:0)
PE(18:1/18:1)
AMPK
ACC
CPT1
CERs
SREBP-1c
FAS
FFAs
DGs
TGs
SCD1
Increase bile acid biosynthesis
Reduce cholesterol synthesis
Regulation of lipid metabolism
TAN supplementation
CEs
CYP7A1
CYP27A1
Anti-obesity
Cholesterol-lowering
Improvement of hepatic steatosis

Table 1. Effect of TAN Supplementation on Body Weight, Energy Intake, and Food Efficiency Ratio in High-Fat Diet-Induced Obese Rats. [a]

Group	ND	HFD	HFD + 0.02% TAN	HFD + 0.04% TAN	HFD + 0.08% TAN
Initial body weight (g)	268.57±12.83^{a}	269.83±13.53^{a}	274.83±16.35^{a}	272.33±18.75^{a}	267.00±6.68^{a}
Final body weight (g)	510.83±19.71^{a}	610.50±25.25^{d}	593.00±16.66^{cd}	581.43±17.19^{bc}	561.50±18.75^{b}
Weight gain (g)	245.38±18.65^{a}	336.50±18.84^{d}	317.00±21.95^{cd}	304.17±18.69^{bc}	290.50±15.40^{b}
Energy intake (kcal/rat/day)	96.74±3.85^{a}	117.56±4.66^{b}	115.05±7.51^{b}	115.52±5.05^{b}	113.36±7.69^{b}
Food efficiency ratio (%) [b]	19.17±3.83^{a}	30.46±2.48^{c}	28.20±2.91^{bc}	26.93±1.74^{b}	25.86±2.30^{b}

[a] The ND and HFD groups for body weight, energy intake and food efficiency ratio in rats were to previously published data.[21] [b] Food efficiency ratio (%) = (daily weight gain ÷ daily food intake) × 100. Results are displayed as mean ± SD (n = 8). The data with different labels (a–d) in rows indicate significant difference ($p < 0.05$).

Table 2. Effect of TAN Supplementation on Relative Organ Weights and Relative Adipose Tissue Weights in High-Fat Diet-Induced Obese Rats. [a]

Group	ND	HFD	HFD + 0.02% TAN	HFD + 0.04% TAN	HFD + 0.08% TAN
Relative organ weights [b]					
Heart (%)	0.28±0.02^{a}	0.27±0.02^{a}	0.29±0.02^{a}	0.27±0.02^{a}	0.28±0.01^{a}
Liver (%)	2.99±0.18^{a}	4.77±0.11^{c}	4.64±0.45^{c}	4.22±0.27^{b}	4.27±0.33^{b}
Spleen (%)	0.16±0.02^{a}	0.16±0.03^{a}	0.16±0.04^{a}	0.15±0.02^{a}	0.14±0.02^{a}
Lung (%)	0.32±0.03^{a}	0.29±0.05^{a}	0.33±0.03^{a}	0.30±0.04^{a}	0.31±0.03^{a}
Kidney (%)	0.62±0.04^{a}	0.59±0.05^{a}	0.60±0.05^{a}	0.61±0.06^{a}	0.63±0.05^{a}
Relative adipose tissue weights [c]					
perirenal adipose (%)	1.83±0.28^{a}	2.73±0.19^{c}	2.36±0.31^{b}	2.36±0.32^{b}	2.16±0.24^{ab}
epididymal adipose (%)	1.37±0.12^{a}	1.80±0.16^{c}	1.64±0.31^{bc}	1.54±0.18^{ab}	1.48±0.14^{ab}
Visceral adipose tissue (%)	3.11±0.31^{a}	4.57±0.55^{c}	3.94±0.35^{b}	3.88±0.38^{b}	3.60±0.24^{ab}

[a] The ND and HFD groups for relative organ weights and relative adipose tissue weights in rats were to previously published data.[21] [b] The relative organ weight was calculated as a percentage of body weight (eg. liver index = liver weight ÷ final body weight ×100). [c] The relative adipose tissue weights were calculated as a percentage of body weight (eg. relative perirenal adipose weight = perirenal adipose weight ÷ final body weight ×100). Relative visceral adipose tissue weights (perirenal adipose tissue weight + epididymal adipose tissue weight) was expressed as a percentage of body weight. Results are displayed as mean ± SD (n = 8). The data with different labels (a–c) in rows indicate significant difference ($p < 0.05$).

Table of Contents Graphic